Carbohydrate Polymers 104 (2014) 158–165

Contents lists available at ScienceDirect

Carbohydrate Polymers

journal homepage: www.elsevier.com/locate/carbpol

Study of osteogenic differentiation of human adipose-derived stem cells (HASCs) on bacterial cellulose

Shanshan Zang[a,1], Qi Zhuo[b,1], Xiao Chang[c], Guixing Qiu[c], Zhihong Wu[c,*], Guang Yang[a,**]

[a] Department of Biomedical Engineering, College of Life Science and Technology, Huazhong University of Science and Technology, Wuhan 430074, China
[b] Department of Orthopaedic Surgery, Chinese PLA General Hospital, Beijing 100853, China
[c] Department of Orthopaedics, Peking Union Medical College Hospital, Beijing 100730, China

ARTICLE INFO

Article history:
Received 5 September 2013
Received in revised form 23 October 2013
Accepted 6 January 2014
Available online 18 January 2014

Keywords:
Bacterial cellulose
Human adipose-derived stem cells
Bone tissue engineering
Biomaterials
Artificial scaffold

ABSTRACT

Bacterial cellulose (BC) has been proposed as a biomaterial applied in biomedical scope due to its good biocompatibility. Recent reports showed that human adipose-derived stem cells (HASCs) have become a new choice to be used as seeding cells in tissue engineering. The objective of this study is to explore the potential of using BC and HASCs as scaffold and seeding cells in bone tissue engineering. The osteogenic differentiation was investigated by Von Kossa, Alizarin Red, ALP cellular staining and RT-PCR. The results showed that HASCs took a successful osteogenic differentiation on BC. Moreover, the *in vivo* animal test also provided the confirmation of the repair ability of BC on damaged bone. In conclusion, the author demonstrates the osteogenic differentiation of HASCs on BC and the feasibility of using BC and HASCs as scaffold and seeding cells in bone tissue engineering.

Crown Copyright © 2014 Published by Elsevier Ltd. All rights reserved.

1. Introduction

Bone tissue engineering has become an important new field of research, the aim of which is the formation and regeneration of injured organs resulted from trauma, surgical resection and congenital deformity corrections (Rodan, 1992; Sommerfeldt & Rubin, 2001). In addition, damages of cartilage such as acute mechanical damage (AMD), affect the structural integrity of the cartilage and cause chondrocyte metabolic dysfunction and death (Schlichting et al., 2011). Tissue engineering has three fundamental components: cells, scaffold and growth factors (Reddi, 1998). Consequently, interests in this research field mainly focus on seed cells and biodegradable scaffold as well as cytokines and microenvironment, which contribute to osteogenesis.

Firstly, the regeneration of mesenchymal tissue needs large numbers of stem cells to serve for tissue engineering (Salgado, Coutinho, & Reis, 2004). Bone marrow mesenchymal stem cells (BMCs) are used for tissue regeneration, but they are not widely applied due to the limited proliferative capacity of terminally differentiated osteoblasts and the morbidity of donor sites (De Ugarte et al., 2003), also their supply is very limited (Bruder, Fink, & Caplan, 1994). However, the recent development in the field of stem cells suggests that human adipose-derived mesenchymal stem cells (HASCs) are the most ideal cell source for tissue engineering applications due to their capability to proliferate and differentiate into adipogenic, osteogenic, chondrogenic and myogenic lineages under appropriate conditions (Gimble, Katz, & Bunnell, 2007; Halvorsen et al., 2001; Huang et al., 2002; Zuk et al., 2001, 2002). The abundance in adipose tissue makes HASCs can be easily obtained through liposuction and expanded (Izadpanah et al., 2006; Mitchell et al., 2006; Mizuno et al., 2002; Nuttall, Patton, Olivera, Nadeau, & Gowen, 1998; Owen & Friedenstein, 1988; Owen et al., 1990). All these advantages make HASCs a major research focus.

Besides the desirable cells, the scaffold is also very important for tissue engineering (Hutmacher, 2000). Organic polymeric materials, such as polylactic acid (PLA), polyglycolic acid (PGA) and poly(lactic-co-glycolic acid) (PLGA) are most widely used, but all of them have serious disadvantages. They show low hydrophilicity, low cell adhesion ability and low mechanical strength. In addition, their acid degradation causes aseptic inflammation easily. Others like natural organic scaffold material have major disadvantages such as low strength, uncontrollable degradation, poor mechanical properties and poor processability. Furthermore, the durability of inorganic synthetic scaffolds is unpredictable and their implantation inhuman body frequently causes rejection (Peter, Miller, Yasko, Yaszemski, & Mikos, 1998; Puppi, Chiellini, Piras, & Chiellini, 2010).

Nanomaterials can combine advantages of different components, so they will attract wide attention as biomaterial in the future (Stylios, Wan, & Giannoudis, 2007). Scaffolds derived

* Corresponding author. Tel.: +86 106 9152809.
** Corresponding author. Tel.: +86 278 7793523.
E-mail addresses: wuzh3000@126.com (Z. Wu), yang_sunny@yahoo.com (G. Yang).
[1] Joint first authors (these authors contributed equally to the work).

0144-8617/$ – see front matter. Crown Copyright © 2014 Published by Elsevier Ltd. All rights reserved.
http://dx.doi.org/10.1016/j.carbpol.2014.01.019

from natural polymers offer greater bioactivity and biocompatibility with mammalian tissues to favor tissue healing, due to their similarity to native extracellular matrix (ECM) components (Aravamudhan et al., 2013). The natural polymers chitosan and alginate represent an attractive material choice for biodegradable implants (Wang, Jamal, Detamore, & Berkland, 2011). Bacterial cellulose (BC) is a nanofiber material built up by *Acetobacter xylinum* (Brown, Willison, & Richardson, 1976). Although its structure is similar, properties of BC are quite different from those of plant cellulose. BC has some unique properties as a novel biomaterial, such as ultrafine structure, high crystallinity and chemical purity, high tensile strength and elastic modulus, high biocompatibility and good biodegradability (Czaja, Young, Kawechi, & Brown, 2007; Helenius et al., 2006; Yamamoto, Horii, & Hirai, 1996). Due to its unique structure and specific properties, as nanofiber scaffold for tissue engineering, BC attracts extensive attention all over the world (Iguchi, Yamanaka, & Budhiono, 2000) and has been used in tissue engineering of cartilage (Svensson et al., 2005), replacements of blood vessels and wound healing process (Czaja, Krystynowicz, Bielecki, & Brown, 2006; Klemm, Schumann, Udhardt, & Marsch, 2001). Besides, BC has excellent physical and chemical properties and biocompatibility. The fiber structure and the composition of bone collagen are consistent in terms of morphology. The microfiber surface modification induces the crystals in a way similar to growth process in bone tissue. These excellent properties make BC a potential scaffold for bone tissue engineering (Burg, Porter, & Kellam, 2000; Hutmacher, 2000; Yasuda et al., 2005).

Here, we show that HASCs and BC can be together used in bone tissue engineering. We investigated the attachment, proliferation and osteogenic differentiation ability of HASCs on BC to evaluate their feasibility for using as seeding cells. Furthermore, BC is shown to be a replacement on damaged bone which exhibits its biocompatibility.

2. Materials and methods

2.1. Preparation of BC

The strain ATCC 53582 of *Acetobacter xylinum* (American Type Culture Collection, Manassas, VA, USA) was cultured in a tray containing Hestrin and Schramm medium in a static culture at 30 °C for 7 days. The optimum medium consisted of (g/L): D-glucose 20, peptone 5, yeast extract 5, Na_2HPO_4 2.7, and citric acid 1.5. BC hydrogel obtained from the medium was soaked in distilled water for 48 h, boiled in 1% NaOH for 30 min and washed by distilled water to a neutral PH. The yeast and peptone were purchased from Beijing Shuangxuan Microbe Culture Medium Products Factoty, PR China, and the reagents were purchased from Sinopharm Chemical Reagent Beijing Co. Ltd., PR China. The resultant BC membrane was placed in NS (Cell Culture Center, CAMS, PR China) and disinfected under damp-heat and high pressure for 20 min. Then, the BC membrane was soaked in a PBS solution (PH 7.4, Cell Culture Center, CAMS, PR China) for 24 h and then in a HASCs medium (Cyagen Bioscience, Inc., USA) for 24 h. SEM (S-3000 N, Hitachi Ltd., Japan) observation was taken to check the ultrafine structure of BC.

2.2. Subculture of HASCs

HASCs were isolated, cultured and characterized by the Institute of Microcirculation, Chinese Academy of Medical Science. Procedures of subculture conform to methods reported previously (Gimble, Katz, & Bunnell, 2007). The adhesion of HASCs was investigated by frozen sectioning/HE staining. The growth pattern and morphology of HASCs on BC was observed by invert phase contrast light microscopy (XDS-1B, Chongqing Optical Instruments Company, PR China).

2.3. Study of osteogenic differentiation and cell evaluation of HASCs on BC

The cultivation of HASCs was divided into four groups (A, B, C and D):

Group A: The HASCs was planted on a BC membrane with an osteogenic induction medium.
Group B: The HASCs was planted on a normal 6-well plate with osteogenic induction medium.
Group C: The HASCs was planted on a BC membrane with a normal HASCs medium.
Group D: The HASCs was planted on a normal 6-well plate with a normal HASCs medium.

After counting, the second or third passage of the cells was inoculated into the four groups as described above. After 24 h, the cells attached to the well. 2 ml of a complete adipose stem cells medium or osteogenic induction medium (consisting of dexamethasone, β-glycerophosphate, and ascorbic acid) was added. The reagents were purchased from Sinopharm Chemical Reagent Beijing Co. Ltd., PR China. Then the cell culture plates were put into the incubator (5% CO_2 at 37 °C), and the medium was changed every 3 days. The growth morphology of HASCs was observed during the process of osteogenic differentiation by an optical microscope on the 1st, 10th and 21st day.

The cultivation was over after 4 weeks, and then the osteogenic differentiation of cells of the four groups (A, B, C, and D) were observed respectively by staining of the following three methods (A, B and C):

A: Von Kossa staining of cells to detect osteogenic differentiation

Samples in each group were rinsed with PBS and fixed in 4% paraformaldehyde (Cell Culture Center, CAMS, PR China) for 1 h at room temperature. Samples were then incubated in 5% silver nitrate (Cell Culture Center, CAMS, PR China) for 30 min in the darkness, rinsed with distilled water and exposed to ultraviolet light for 1 h.

B: Alizarin Red staining of cells to detect osteogenic differentiation

Samples in each group were rinsed with PBS and fixed in 4% paraformaldehyde for 1 h. Samples were incubated with 1% alizarinered S solution (Cell Culture Center, CAMS, PR China) for 10 min at room temperature, then washed with running tap water for 5 min and left to dry.

C: Alkaline Phosphatase staining of cells to detect osteogenic differentiation

Samples in each group were rinsed with PBS and fixed in 4% paraformaldehyde for 2 min, and rinsed twice by TBST (20 mM Tris–HCl, 0.15 mM NaCl, 0.05% Tween-20, pH 7.4, Sinopharm Chemical Reagent Beijing Co. Ltd., PR China). Then, they were incubated in the NBT/BCIP (Cell Culture Center, CAMS, PR China) ready-to-use solution in the darkness at room temperature for 20 min according to the manufacturer's instruction.

Fig. 1. Animal surgery.

2.4. Osteogenic differentiation and gene expression of HASCs on BC

The cultivation of HASCs was divided into four groups (A, B, C and D) and the methodology of culturing was the same as mentioned above in Section 2.3.

Total RNA was extracted from cells cultured on BC discs for 14 and 28 days after seeding respectively, using a TRIzol Reagent (Cyagen Bioscience, Inc., USA) according to the manufacturer's instruction. The concentration of RNA was determined from the optical absorbance at 260 nm of the extract. Complementary DNA (cDNA) was synthesized using Reverse Transcriptase System. Real-time PCR was performed using PTC DNA Engine Systems (BioTek Instruments, Inc., USA). PCR Mix was used in each reaction. Reactions were performed with 40 cycles as follows: 94 °C for 30 s, annealing temperature for 30 sand 72 °C for 30 s. Markers for osteogenic differentiation: Osteopontin, Osteocalcin and Alkaline Phosphatase were evaluated, while GAPDH gene served as the control (sequences of primers, individual annealing temperature and amplicon lengths were shown in Table 1). PCR products were resolved using conventional agarose gel electrophoresis. Images were processed with Quantity One-Version 4.0 software, under the same parameters. Gray-scale measurement of the target bands (optical density of target gene) was divided by the measurement of internal reference electrophoresis band (optical density of GAPDH). The ratio was used as semi-quantitative detection value of amplified fragment (light density of target gene/optical density of GAPDH).

2.5. Animal test

All surgeries were performed under a protocol approved by the Peking Union Medical College Hospital Animal Care Committee. An ulna damaged rabbit model *in vivo* was employed in the current study (Fig. 1). The test was divided into two groups: ulna defects with no implants were chosen as control while ulna defects with scaffold and seeding cells were in the experimental group. Two circular defects, 3 mm in diameter, were created at the ulna on each rabbit. Animals were anesthetized with a ketamine/xylazine mixture (135 mg/kg and 15 mg/kg, Sinopharm Chemical Reagent Beijing Co. Ltd., PR China). Briefly, an 8–10 mm incision was made along the sagittal suture by scalpel blade. A skin flap was then raised to expose the underlying bone and two holes with 3 mm diameter were drilled. The defect was filled with a scaffold loaded with cells based on the experimental design. HASCs at a density of 1.0×10^6 cells/scaffold were loaded into each pre-hydrated scaffold 5 min before implantation. After the surgery, the rabbit was raised for 8 weeks and then imaged using a microradiography unit (Faxitron X-ray LX 60, USA). X-ray photographs were taken at 24 kV for 8 s.

2.6. Statistical analysis

All PCR experiments were repeated 3 times and the scanning images of the electrophoresis gel were measured. Ratio of the obtained gray-scale of target band to that of the internal reference electrophoretic band was regarded as the semi-quantitative measurement value of the target fragment, and the average value of three times was taken as the final. Experimental data were analyzed with SPSS15.0 software. To determine whether the data were normally distributed, t test and rank sum test were conducted and correlation was analyzed for the data. If $P < 0.05$, data were statistically plain; if $P < 0.01$, data were statistically significant.

3. Results

3.1. Process of cellulose formation

According to our previous research (Shi et al., 2012), sub-elementary fibrils were firstly assembled to form microfibrils ($d = 3$–4 nm) and further polymerized to form ribbons ($d = 30$–50 nm), which finally developed into a hyperfine network structure through interactive interweaving. ESEM images of the dried BC membrane showed that they formed densely and finely branched nanolevel networks in the planar direction and microfibrils were 40 nm in diameter (Fig. 2).

3.2. Study of osteogenic differentiation and cell evaluation of HASCs in BC

According to our previous research (Fu et al., 2012), through the measurement of culture HASCs on BC to study the proliferation of HASCs on BC, the cells formed a coherent layer on BC; HASCs grew well on BC and BC showed a good biocompatibility to HASCs. HASCs proliferated fast. Nine days later, the proliferation showed a plateau phase. HASCs were fibroblast-shaped on the BC film and formed a single layer. The frozen section/HE staining of HASCs–BC complex exhibited a continuous layer, which demonstrated a nice proliferation of the stem cells on the BC film. The adhesion of HASCs to the BC film was also good (Fig. 3).

3.2.1. Morphological changes during the osteogenic differentiation of HASCs

During osteogenic induction, HASCs attached to the well prismatically and ovally for a long time, and the cytoplasm could be barely seen. In later stages, the cells grew quickly and covered the bottom in 10 days, their sizes were short spindle-like and polygonal. On prolonging the induction time, the cells aggregated and formed colonies and the morphology of the cells changed clearly into cubical and conical with visible cytoplasm. Osteogenic cells appeared till the 21st day. The color of the cytoplast turned dark with visible coarse particles. The nuclear of HASCs was clear, and secretion of extracellular matrix increased gradually. Many filopodias protruded from the cytoplasm and opaque mineralized nodules could be seen clearly (Fig. 4).

3.2.2. Von Kossa staining to detect osteogenic differentiation

With a silver reduction technology, Von Kossa staining analyzes calcium deposition in the fixed cell samples. Stained by argyrophilic dye, calcium ions are replaced by silver ions. Under strong

Table 1
Sequences of primers and real-time PCR conditions.

Gene	Primers (F = forward, R = reverse)	Amplicon size (bp)	Annealing temperature (°C)
Osteopontin	F: 5′-TGGCTAAACCCTGACCCATCTC-3′ R: 5′-CTTCCCACGGCTGTCCCAATC-3′	498	60
Osteocalcin	F: 5′-GCCACCGAGACACCATGAGA-3′ R: 5′-AGCAGAGCGACACCCTAGACC-3′	331	54
Alkaline Phosphatase	F: 5′-ACGGCGTCCACGAGCAGAACT-3′ R: 5′-GCCTCTGGGTCTGGAGAAATACG-3′	492	60
GAPDH	F: 5′-CATGAGAAGTATGACAACAGCCT-3′ R: 5′-AGTCCTTCCACGATACCAAAGT-3′	113	54

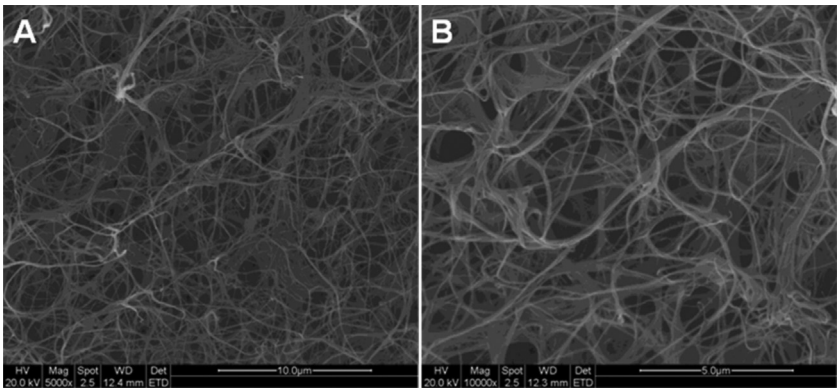

Fig. 2. SEM pictures of BC: (A) the scale bar equals to 10 μm; (B) the scale bar equals to 5 μm.

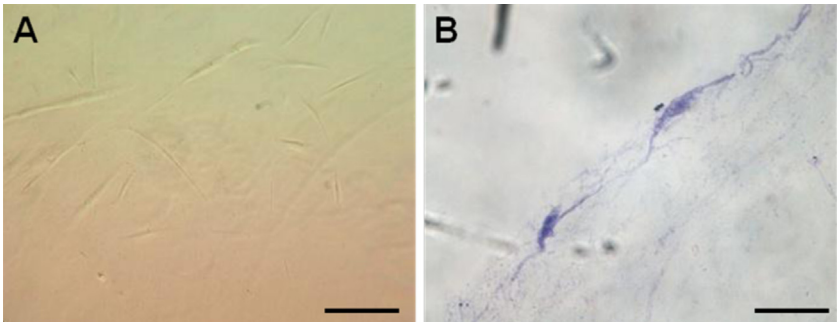

Fig. 3. Microphotographs of HASCs culturing on BC: (A) after cultured for 9 days, the cells formed a layer on the BC surface. The scale bar equals to 50 μm; (B) HE staining of frozen section of HASCs–BC complex. The scale bar equals to 200 μm.

light, silver ions are reduced and the sedimentation is displayed in black. The result showed that groups A and B had a significant positive reaction, demonstrating that a large number of black cells contained mineralized material. But, there were no significant differences between the two groups. With an ordinary culture medium, HASCs of groups C and D showed a negative reaction, but small black particles were barely visible in group C (Fig. 5I).

3.2.3. *Alizarin Red staining to detect osteogenic differentiation*

Alizarin Red staining is achieved by the formation of a colored complex between an Alizarin Red and calcium; this complex identifies the calcium component in cells. The result showed that, with Alizarin Red staining, groups A and B witnessed a large number of calcium deposits in positive cells without significant differences between the two groups. However, there was no positive reaction in group C or D (Fig. 5II).

3.2.4. *Alkaline Phosphatase staining to detect osteogenic differentiation*

Alkaline Phosphatase staining is a technique with which Toluidine blue bromochloromethane indole phosphate is catalyzed by Alkaline Phosphatase; the former then reduces N-nitro-blue tetrazolium to a purple or blue-black precipitate. Alkaline Phosphatase is a specific enzyme of osteoblasts, so its expression can indicate

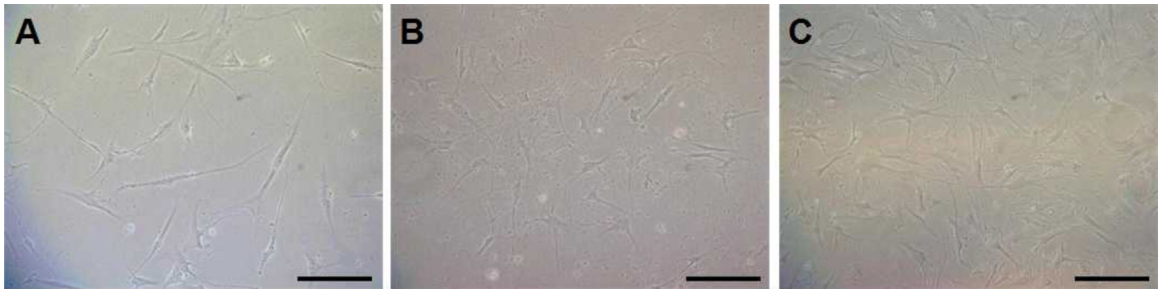

Fig. 4. Morphologic changes during osteogenic differentiation of HASCs: (A) 24 h; (B) 10 d; (C) 21 d (the scale bar equals to 50 μm).

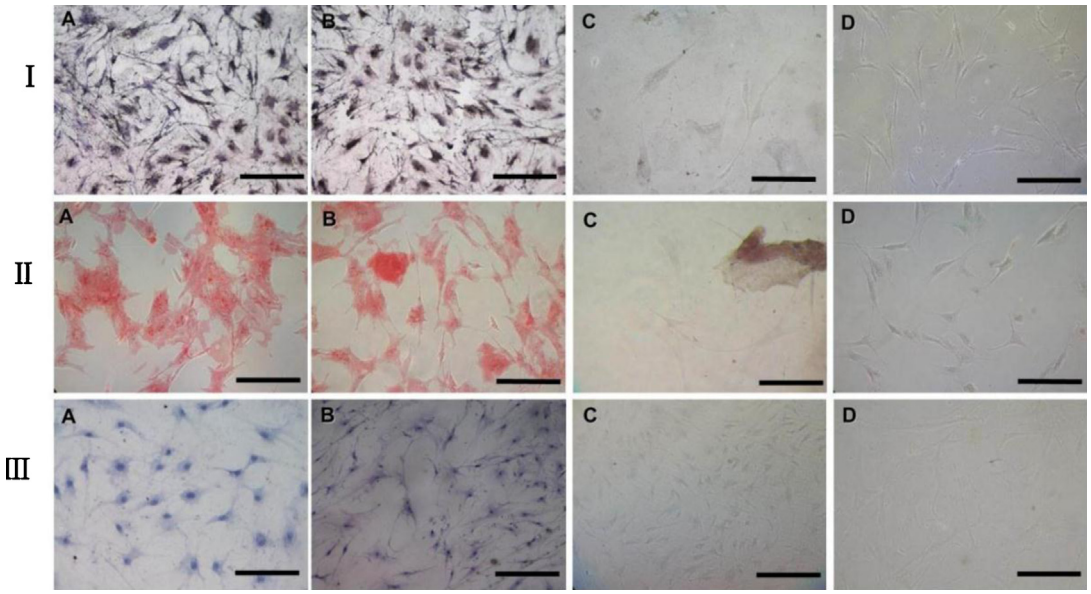

Fig. 5. Results of different staining: (group A) the HASCs was planted on a BC membrane with an osteogenic induction medium; (group B) the HASCs was planted on a normal 6-well plate with osteogenic induction medium; (group C) the HASCs was planted on a BC membrane with a normal HASCs medium; (group D) the HASCs was planted on a normal 6-well plate with a normal HASCs medium. Von Kossa staining of HASCs (I) was cultured in osteogenic and control media at 4 w (the scale bar equals to 50 μm): (A) group A; (B) group B; (C) group C; (D) group D. Alizarin Red staining of HASCs (II) in osteogenic or control medium and on BC membrane on plastic plate at 4 w (the scale bar equals to 50 μm): (A) group A; (B) group B; (C) group C; (D) group D. ALP staining of HASCs (III) in osteogenic or control medium and on BC membrane on plastic plate at 4 w (the scale bar equals to 50 μm): (A) group A; (B) group B; (C) group C; (D) group D.

osteogenic differentiation. The result showed that there were blue-black stained cytoplasm and dark blue nucleus in groups A and B and there were no significant differences. The cytoplasm of group C was light blue, but group D showed a negative reaction (Fig. 5III).

3.3. Osteogenic differentiation and gene expression of HASCs on BC

The average ratio of three times of each gene gray scale to internal reference GAPDH was taken as the final semi-quantitative measurement of fragment values, and we compared to each gene expression in different tissues.

3.3.1. Expression of Osteopontin mRNA in cells

3.3.1.1. Comparison of Osteopontin mRNA expression in different cells. In the first two weeks, there was no obvious Osteopontin mRNA band indicating intracellular expression among four groups. Therefore, there was no statistical significance in gray level differences. However, 4 weeks later, there was clear Osteopontin expression of osteogenic HASCs growing in BC membrane and in normal 6-well plates, and statistical significance of the gray-scale difference was obvious ($P < 0.05$). However, there was no clear expression of Osteopontin in the two groups of cells cultured in normal medium.

3.3.1.2. Comparison of expression of Osteopontin mRNA at different times. In the 2nd week, two kinds of osteogenic cells did not have Osteopontin mRNA. However, in the 4th week, there was obvious Osteopontin gene expression, but there was no clear Osteopontin gene expression of cells in normal medium (Fig. 6A).

3.3.2. Expression of Osteocalcin mRNA in cells

3.3.2.1. Comparison of Osteocalcin mRNA expression in different cells. In first two weeks, there was no obvious Osteocalcin mRNA band indicating intracellular expression among four groups. Therefore, there was no statistical significance in gray level differences. However, 4 weeks later, there was a little Osteocalcin expression of osteogenic HASCs growing in BC membrane and in normal 6-well plates, so statistical significance of the gray-scale difference was plain ($P > 0.05$). However, there was no obvious expression of Osteocalcin in the two groups of cells cultured in normal medium.

3.3.2.2. Comparison of expression of Osteocalcin mRNA at different times. In the 2nd week, two kinds of osteogenic cells did not have Osteocalcin mRNA. However, in the 4th week, there was tiny Osteocalcin gene expression, but there was no obvious Osteocalcin gene expression of cells in normal medium (Fig. 6B).

3.3.3. Expression of Alkaline Phosphatase mRNA in cells

3.3.3.1. Comparison of Alkaline Phosphatase mRNA expression in different cells. In the 2nd week, there were obvious Alkaline Phosphatase bands indicating intracellular expression in four groups. There was statistical significance ($P < 0.05$) between osteogenic HASCs growing in BC membrane and in normal 6-well plates. However, there was no statistical significance ($P > 0.05$) between normal HASCs growing in BC membrane and in normal 6-well plates. In the 2nd week, there were statistically significant differences ($P < 0.001$) in Alkaline Phosphatase expression among all groups growing in the same vector but in different cell culture mediums.

In the 4th week, there was no statistical significance ($P > 0.05$) between osteogenic HASCs growing in BC membrane and in normal 6-well plates. There was no statistical significance ($P > 0.05$) between normal HASCs growing in BC membrane and in normal 6-well plates. At the same time, statistically significant differences ($P < 0.001$) in Alkaline Phosphatase expression among all groups growing in the same vector but in different cell culture mediums still existed.

3.3.3.2. Comparison of expression of Alkaline Phosphatase mRNA at different times. Alkaline Phosphatase mRNA expressions in the four experimental cells decreased from the 2nd week to the 4th week. There were significant differences ($P < 0.001$) before and after the change in each group (Fig. 6C).

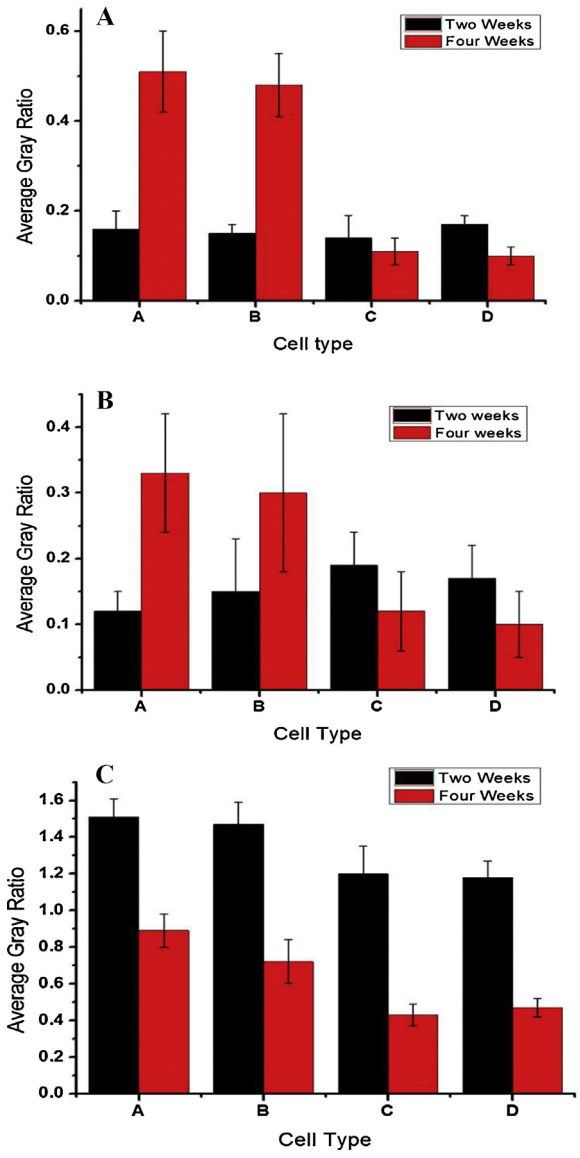

Fig. 6. Comparison of mRNA of different genes at different times: (group A) the HASCs was planted on a BC membrane with an osteogenic induction medium; (group B) the HASCs was planted on a normal 6-well plate with osteogenic induction medium; (group C) the HASCs was planted on a BC membrane with a normal HASCs medium; (group D) the HASCs was planted on a normal 6-well plate with a normal HASCs medium: (A) Osteopontin in the 2nd and 4th weeks; (B) Osteocalcin at 2nd and 4th weeks; (C) Alkaline Phosphatase at 2nd and 4th weeks.

3.3.4. Correlation of Osteopontin, Osteocalcin and Alkaline Phosphatase expression

In the 4th week, three genes mentioned above in the cells had statistically positive correlation. Osteopontin and Osteocalcin were positively correlated in expression ($r = 0.998$, $P = 0.002$) (Fig. 7, the red line). Osteopontin and Alkaline Phosphatase were correlated in expression ($r = 0.959$, $P = 0.04$) (Fig. 7, the black line). Osteocalcin and Alkaline Phosphatase were correlated in expression ($r = 0.965$, $P = 0.04$) (Fig. 7, the blue line).

3.4. Animal test

New bone formation at the ulna defect site was evaluated by X-ray radiological examination 8 weeks after the surgery. The defects filled with scaffold and cells showed scattered mineralized spots, while less self-repair mineralization was observed in the control

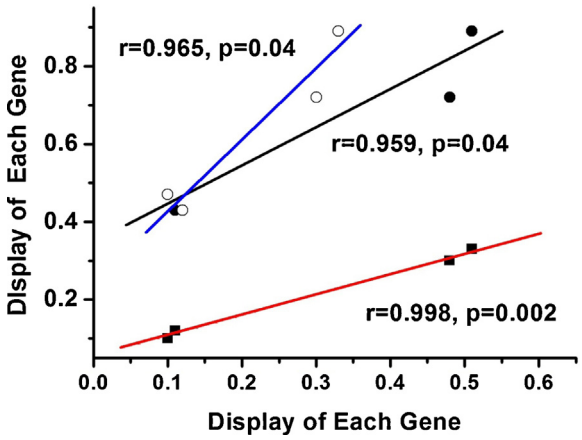

Fig. 7. Correlation of expression between two genes: (the red line) correlation of Osteopontin and Osteocalcin expression in the 4th week; (the black line) correlation of Osteopontin and Alkaline Phosphatase expression in the 4th week; (the blue line) correlation of Osteocalcin and Alkaline Phosphatase expression in the 4th week. (For interpretation of the references to color in this figure legend, the reader is referred to the web version of the article.)

group. No obvious difference of mineralized tissue in quantity between the experiment group and control group (Fig. 8).

4. Discussions

Reconstruction of bone defect caused by trauma, infection, tumor resection and abnormal growth has always been a problem in the orthopedic field. So it is very necessary to explore substitutes for bone tissue engineering, including filling material used for large bone reconstruction. Traditional treatments for bone defects include autogenous bone graft, allogenous bone graft and artificial bone graft. Supply source of autologous bone is limited, and the taking of bone surgery will bring additional pain to the patient; heterologous bone is with antigenicity, and severe immune rejection leads to implant failure and risk of cross infection; although regenerative medicine research has made significant progress in orthopedics in recent years, current treatments, including bone graft, still has many limitations. In addition, although great progress in bone substitutes, the materials science has still not developed a mature and complete bone substitute. Most injuries associated with bone are difficult to heal or cannot be completely treated.

Results of the experiment showed that statically cultured BC formed a pellicle. This pellicle with fine, highly entangled nanofibrils was composed of about 99% water which allowed room for cell ingrowth and proliferation. And adding a certain concentration of dexamethasone, β-glycerophosphate and ascorbic acid medium could induce HASCs to osteogenic cell differentiation. Induction presented significant changes in cell morphology and extracellular matrix deposition.

In the 4th week, cells in each group were stained to detect calcium deposition and ALP matrix expression. Results of groups A and B in Von Kossa, Alizarin Red and ALP staining showed a significant positive reaction. However, in group C in ALP staining, cytoplasm seemed to be weak blue. Groups C and D were negative staining.

Bone-related gene expression was detected by RT-PCR: in the 2nd and 4th weeks, positive ALP was expressed in the cells of all four groups, but osteogenic differentiation in groups A and B was significantly higher than that of ordinary media groups C and D. For groups A and B, whether planted in BC membrane or in the common culture, ALP expression was not significantly different. In the 2nd week, ALP expression of group A was higher than that of group B, which was statistically significant. This conclusion was adequate for the expression of OP and OC. In the 2nd week, OC and

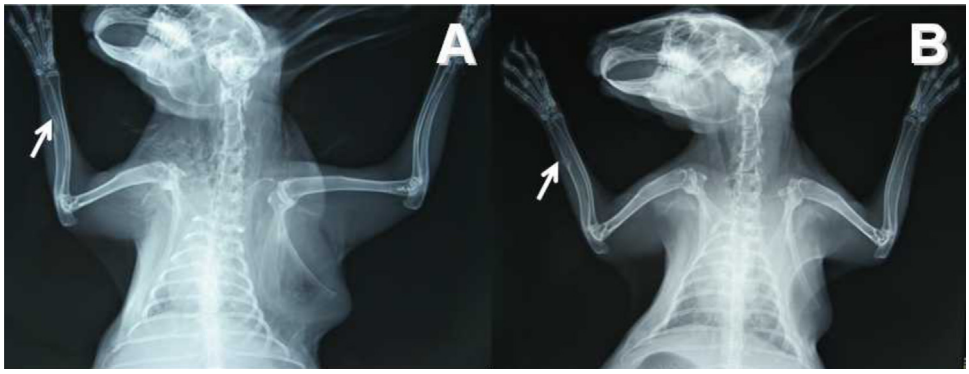

Fig. 8. X-ray test of surgery *in vivo*: (A) photos of self-repair; (B) photos of BC repair.

OP had no significant expression in all four experimental groups, but a visible expression of OP bands appeared in the 4th week, and OC band appeared relatively indistinct. In the 4th week, OC and OP had no significant difference between groups A and B, though the gray value of OP bands had some significant differences between groups A and B. In addition, related studies on expression suggested that the expression of OC, OP and ALP had strong positive correlation.

Osteogenic supplements include a certain proportion of dexamethasone, ascorbic acid and β-glycerophosphate. This classical program of osteogenic supplements induct bone formation quickly, usually manifested at changes in cell morphology, the increase of ALP, OP and OC expression and the formation of mineralized extracellular matrix (Jaiswal, Haynesworth, Caplan, & Bruder, 1997). The presence of dexamethasone not only promotes the growth and differentiation of stromal cells, but also impels bone cells to adjust insulin-like growth factor and the synthesis of extracellular matrix. Ascorbic acid helps extracellular matrix deposition. β-glycerophosphate guides bone osteoblasts and improves the deposition of calcium phosphate (Coelho & Fernandes, 2000).

The development of cells to form bone can be divided into three stages: cell proliferation phase; extracellular matrix secretion, deposition and maturation; and mineralization of the extracellular matrix (Owen et al., 1990). In the process of osteogenic differentiation, different states of cells are highly related to gene expression in different stages. ALP is the early sign in the process of osteogenic differentiation. The increase of mRNA expression promotes secretion of phosphate in local content, further promoting extracellular matrix maturation and mineralization (Zuk et al., 2001). OP is a phosphorylated glycoprotein secreted by osteoblasts which exercises the function of extracellular matrix mineralization during bone formation (Beck, Zerler, & Moran, 2000). OC is an osteoblast-specific gene. It is generally believed that it has expression at the end of osteogenic differentiation (Lee et al., 2007).

With the program of dexamethasone, ascorbic acid and β-glycerophosphate in present study, stem cells induced differentiation into bone successfully in the general cell culture and BC membrane. Obvious morphological changes were observed at the 10th day in the osteogenic induction medium. On the 21st day, deposition of extracellular matrix and bright calcium phosphate could be seen. HASCs changed from long spindle shape into square or polygon. RT-PCR results showed ALP expression was significant over 2 weeks and declined in the 4th week. OC and OP expression was not obvious over two weeks, while there was a certain expression in the 4th week. In the 4th week, Von Kossa and Alizarin Red staining of calcium nodules and ALP staining cells were significantly positive. It was consistent with the time pattern of gene expression during bone formation mentioned in the same literature: enzyme activity of ALP causing the increase of substrate phosphorylation may induce transcription and expression of OP and OC, which may be the adjusting mechanism in the process of bone formation.

Although expression of ALP, OP had some significant differences between the BC membrane and normal cell cultures during the HASCs osteogenic differentiation, the difference was not stable. Maybe the structure of BC itself could not provide additional advantage of HASCs differentiation, though the experiment showed that it had excellent biocompatibility. Another possible reason is that the BC membrane had strong ability of water retention. All experimental films were immersed in PBS for 24 h and soaked in HASCs basic medium for 24 h before the experiment. When HASCs were planted on its surface and induced transformation medium was added, cells planted in BC could not be guaranteed to fully access effective differentiation microenvironment. This is an overlooked detail and will be improved in future experimental studies. In spite of this, results show the excellent biocompatibility of BC membrane and the great differentiation potential of HASCs in this new type of biological material. Moreover, through the basic animal test, it could be seen that using BC and HASCs as scaffold and seeding cells could improve the repair of damaged bone *in vivo* compared to the result of self-repair without causing inflammation response.

In addition, composite material of BC and hydroxyapatite (HAp) is synthesized and characterized (Grande, Torres, Gomez, & Bañó, 2009; Hong et al., 2006; Hutchens, Benson, Evans, O'Neill, & Rawn, 2006; Wan et al., 2006). HAp crystals are very similar to natural bone, which has been proved by researches. With citrate concentrations comparable to those in body fluids, HAp nanocrystals with sizes and morphologies similar to those in avian and bovine bones have been produced (Hu et al., 2011). When combined with BC, HAp used for the artificial bone tissue engineering and development of scaffold is very attractive in the future. It also provides the direction to use BC membranes in the future. It means making full use of advantages of different materials to develop bone tissue engineering materials in possession of the ideal bone induction, conduction, and the similarity to natural bone in strength, mechanical and processing properties.

5. Conclusions

There is a definite need for specific design of scaffold architecture that can better match the structural organization of surrounding tissues. A well-supported seed cell is also needed to improve the growth of new cells in the damaged tissue. In summary, through the cell test, the biocompatibility of BC with fine 3D nanonetwork leads to good adhesion, growth and proliferation of HASCs and HASCs can be differentiated into an osteogenic lineage, which is the key factor of regeneration of new bone in a three-dimensional BC scaffold. Furthermore, with BC and HASCs used as scaffold and seed cells, their combination can be well implanted into a damaged bone model. Application of these results to *in vivo*

models may result in the development of a useful tool in the field of bone tissue engineering.

Acknowledgments

This work was supported by the National Natural Science Foundation of P.R. China (21074041, 81201404).

References

Aravamudhan, A., Ramos, D. M., Nip, J., Harmon, M. D., James, R., Deng, M., et al. (2013). Cellulose and collagen derived micro-nano structured scaffolds for bone tissue engineering. *Journal of Biomedical Nanotechnology*, *9*(4), 719–731.

Beck, G. R., Zerler, B., & Moran, E. (2000). Phosphate is a specific signal for induction of osteopontin gene expression. *Proceedings of the National Academy of Science*, *97*(15), 8352–8357.

Brown, R. M., Willison, J. H., & Richardson, C. L. (1976). Cellulose biosynthesis in *Acetobacter xylinum*: Visualization of the site of synthesis and direct measurement of the in vivo process. *Proceedings of the National Academy of Science*, *73*(12), 4565–4569.

Bruder, S. P., Fink, D. J., & Caplan, A. I. (1994). Mesenchymal stem cells in bone development, bone repair, and skeletal regeneration therapy. *Journal of Cellular Biochemistry*, *56*(3), 283–294.

Burg, K. J. L., Porter, S., & Kellam, J. F. (2000). Biomaterial developments for bone tissue engineering. *Biomaterials*, *21*(23), 2347–2359.

Coelho, M. J., & Fernandes, M. H. (2000). Human bone cell cultures in biocompatibility testing. Part II: Effect of ascorbic acid, β-glycerophosphate and dexamethasone on osteoblastic differentiation. *Biomaterials*, *21*(11), 1095–1102.

Czaja, W., Krystynowicz, A., Bielecki, S., & Brown, R. M. (2006). Microbial cellulose—The natural power to heal wounds. *Biomaterials*, *27*(2), 145–151.

Czaja, W. K., Young, D. J., Kawecki, M., & Brown, R. M. (2007). The future prospects of microbial cellulose in biomedical applications. *Biomacromolecules*, *8*(1), 1–12.

De Ugarte, D. A., Morizono, K., Elbarbary, A., Alfonso, Z., Zuk, P. A., Zhu, M., et al. (2003). Comparison of multi-lineage cells from human adipose tissue and bone marrow. *Cells Tissues Organs*, *174*(3), 101–109.

Fu, L. N., Zhang, Y., Li, C., Wu, Z. H., Zhuo, Q., Huang, X., et al. (2012). Skin tissue repair materials from bacterial cellulose by a multilayer fermentation method. *Journal of Materials Chemistry*, *22*(24), 12349–12357.

Gimble, J. M., Katz, A. J., & Bunnell, B. A. (2007). Adipose-derived stem cells for regenerative medicine. *Circulation Research*, *100*(9), 1249–1260.

Grande, C. J., Torres, F. G., Gomez, C. M., & Bañó, M. C. (2009). Nanocomposites of bacterial cellulose/hydroxyapatite for biomedical applications. *Acta Biomaterialia*, *5*(5), 1605–1615.

Halvorsen, Y. D. C., Franklin, D., Bond, A. L., Hitt, D. C., Auchter, C., Boskey, A. L., et al. (2001). Extracellular matrix mineralization and osteoblast gene expression by human adipose tissue-derived stromal cells. *Tissue Engineering*, *7*(6), 729–741.

Helenius, G., Backdahl, H., Bodin, A., Nannmark, U., Gatenholm, P., & Risberg, B. (2006). In vivo biocompatibility of bacterial cellulose. *Journal of Biomedical Materials Research Part A*, *76*(2), 431–438.

Hong, L., Wang, Y. L., Jia, S. R., Huang, Y., Gao, C., & Wan, Y. Z. (2006). Hydroxyapatite/bacterial cellulose composites synthesized via a biomimetic route. *Materials Letters*, *60*(13), 1710–1713.

Hu, Y. Y., Liu, X. P., Ma, X., Rawal, A., Prozorov, T., Akinc, M., et al. (2011). Biomimetic self-assembling copolymer–hydroxyapatite nanocomposites with the nanocrystal size controlled by citrate. *Chemistry of Materials*, *23*(9), 2481–3249.

Huang, J. I., Beanes, S. R., Zhu, M., Lorenz, H. P., Hedrick, M. H., & Benhaim, P. (2002). Rat extramedullary adipose tissue as a source of osteochondrogenic progenitor cells. *Plastic and Reconstructive Surgery*, *109*(3), 1033–1041.

Hutchens, S. A., Benson, R. S., Evans, B. R., O'Neill, H. M., & Rawn, C. J. (2006). Biomimetic synthesis of calcium-deficient hydroxyapatite in a natural hydrogel. *Biomaterials*, *27*(26), 4661–4670.

Hutmacher, D. W. (2000). Scaffolds in tissue engineering bone and cartilage. *Biomaterials*, *21*(24), 2529–2543.

Iguchi, M., Yamanaka, S., & Budhiono, A. (2000). Bacterial cellulose—A masterpiece of nature's arts. *Journal of Materials Science*, *35*(2), 261–270.

Izadpanah, R., Trygg, C., Patel, B., Kriedt, C., Dufour, J., Gimble, J. M., et al. (2006). Biologic properties of mesenchymal stem cells derived from bone marrow and adipose tissue. *Journal of Cellular Biochemistry*, *99*(5), 1285–1297.

Jaiswal, N., Haynesworth, S. E., Caplan, A. I., & Bruder, S. P. (1997). Osteogenic differentiation of purified, culture-expanded human mesenchymal stem cells in vitro. *Journal of Cellular Biochemistry*, *64*(2), 295–312.

Klemm, D., Schumann, D., Udhardt, U., & Marsch, S. (2001). Bacterial synthesized cellulose—Artificial blood vessels for microsurgery. *Progress in Polymer Science*, *26*(9), 1561–1603.

Lee, N. K., Sowa, H., Hinoi, E., Ferron, M., Ahn, J. D., Confavreux, C., et al. (2007). Endocrine regulation of energy metabolism by the skeleton. *Cell*, *130*(3), 456–469.

Mitchell, J. B., McIntosh, K., Zvonic, S., Garrett, S., Floyd, Z. E., Kloster, A., et al. (2006). Immunophenotype of human adipose-derived cells: Temporal changes in stromal-associated and stem cell-associated markers. *Stem Cells*, *24*(2), 376–385.

Mizuno, H., Zuk, P. A., Zhu, M., Lorenz, P. H., Benhaim, P., & Hedrick, M. H. (2002). Myogenic differentiation by human processed lipoaspirate cells. *Plastic and Reconstructive Surgery*, *109*(1), 199–209.

Nuttall, M. E., Patton, A. J., Olivera, D. L., Nadeau, D. P., & Gowen, M. (1998). Human trabecular bone cells are able to express both osteoblastic and adipocytic phenotype: Implications for osteopenic disorders. *Journal of Bone and Mineral Research*, *13*(3), 371–382.

Owen, T. A., Aronow, M., Shalhoub, V., Barone, L. M., Wilming, L., Tassinari, M. S., et al. (1990). Progressive development of the rat osteoblast phenotype in vitro: Reciprocal relationships in expression of genes associated with osteoblast proliferation and differentiation during formation of the bone extracellular matrix. *Journal of Cellular Physiology*, *43*(3), 420–430.

Owen, M., & Friedenstein, A. J. (1988). Stromal stem cells: Marrow-derived osteogenic precursors. *Cell and Molecular Biology of Vertebrate Hard Tissues*, *136*, 42–60.

Peter, S. J., Miller, M. J., Yasko, A. W., Yaszemski, M. J., & Mikos, A. G. (1998). Polymer concepts in tissue engineering. *Journal of Biomedical Materials Research*, *43*(4), 422–427.

Puppi, D., Chiellini, F., Piras, A. M., & Chiellini, E. (2010). Polymeric materials for bone and cartilage repair. *Progress in Polymer Science*, *35*(4), 403–440.

Reddi, A. H. (1998). Role of morphogenetic proteins in skeletal tissue engineering and regeneration. *Nature Biotechnology*, *16*(3), 247–252.

Rodan, G. A. (1992). Introduction to bone biology. *Bone*, *13*, 3–6.

Salgado, A. J., Coutinho, O. P., & Reis, R. L. (2004). Bone tissue engineering: State of the art and future trends. *Macromolecular Bioscience*, *4*(8), 743–765.

Schlichting, K. E., Copeland-Johnson, T. M., Goodman, M., Lipert, R. J., Prozorov, T., Liu, X. P., et al. (2011). Synthesis of a novel photopolymerized nanocomposite hydrogel for treatment of acute mechanical damage to cartilage. *Acta Biomaterialia*, *7*(8), 3094–3100.

Shi, Z. J., Zang, S. S., Jiang, F., Huang, L., Lu, D., Ma, Y. G., et al. (2012). In situ nano-assembly of bacterial cellulose–polyaniline composites. *RSC Advances*, *2*(3), 1040–1046.

Sommerfeldt, D., & Rubin, C. (2001). Biology of bone and how it orchestrates the form and function of the skeleton. *European Spine Journal*, *10*(2), 86–95.

Stylios, G., Wan, T., & Giannoudis, P. (2007). Present status and future potential of enhancing bone healing using nanotechnology. *Injury*, *38*(1), 63–74.

Svensson, A., Nicklasson, E., Harrah, T., Panilaitis, B., Kaplan, D. L., Brittberg, M., et al. (2005). Bacterial cellulose as a potential scaffold for tissue engineering of cartilage. *Biomaterials*, *26*(4), 419–431.

Wan, Y. Z., Hong, L., Jia, S. R., Huang, Y., Zhu, Y., Wang, Y. L., et al. (2006). Synthesis and characterization of hydroxyapatite–bacterial cellulose nanocomposites. *Composites Science and Technology*, *66*(11), 1825–1832.

Wang, Q., Jamal, S., Detamore, M. S., & Berkland, C. (2011). PLGA-chitosan/PLGA-alginate nanoparticle blends as biodegradable colloidal gels for seeding human umbilical cord mesenchymal stem cells. *Journal of Biomedical Materials Research Part A*, *96*(3), 520–527.

Yamamoto, H., Horii, F., & Hirai, A. (1996). In situ crystallization of bacterial cellulose II. Influences of different polymeric additives on the formation of cellulose I_α and I_β at the early stage of incubation. *Cellulose*, *3*(1), 229–242.

Yasuda, K., Gong, J. P., Katsuyama, Y., Nakayama, A., Tanabe, Y., Kondo, E., et al. (2005). Biomechanical properties of high-toughness double network hydrogels. *Biomaterials*, *26*(21), 4468–4475.

Zuk, P. A., Zhu, M., Ashjian, P., De Ugarte, D. A., Huang, J. I., Mizuno, H., et al. (2002). Human adipose tissue is a source of multipotent stem cells. *Molecular Biology of the Cell*, *13*(12), 4279–4295.

Zuk, P. A., Zhu, M., Mizuno, H., Huang, J. I., Futrell, J. W., Katz, A. J., et al. (2001). Multilineage cells from human adipose tissue: Implications for cell-based therapies. *Tissue Engineering*, *7*(2), 211–228.